

Hot-Electron-Induced Dissociation of H₂ on Gold Nanoparticles Supported on SiO₂

Shaunak Mukherjee,^{1,‡,§} Linan Zhou,^{1,‡,§} Amanda M. Goodman,^{1,‡} Nicolas Large,^{#,‡} Ciceron Ayala-Orozco,^{1,‡} Yu Zhang,^{‡,‡} Peter Nordlander,^{*,†,‡,‡} and Naomi J. Halas^{*,1,†,‡,‡}

¹Department of Chemistry, [†]Department of Physics and Astronomy, [#]Department of Electrical and Computer Engineering, and [‡]Laboratory for Nanophotonics, Rice University, 6100 Main Street, Houston, Texas 77005, United States

S Supporting Information

ABSTRACT: Hot-electron-induced photodissociation of H₂ was demonstrated on small Au nanoparticles (AuNPs) supported on SiO₂. The rate of dissociation of H₂ was found to be almost 2 orders of magnitude higher than that observed on equivalently prepared AuNPs on TiO₂. The rate of H₂ dissociation was found to be linearly dependent on illumination intensity with a wavelength dependence resembling the absorption spectrum of the plasmon of the AuNPs. This result provides strong additional support for the hot-electron-induced mechanism for H₂ dissociation in this photocatalytic system.

In the field of heterogeneous catalysis, noble metal nanoparticles (NPs) have emerged as a new breed of photocatalysts enabling chemical reactions^{1–3} such as diatomic molecular dissociation,^{4–7} water splitting,^{8,9} and organic liquid-phase chemical reactions^{10,11} by a plasmon-induced, hot-electron-based mechanism.^{5,12–14} The unique ability to perform chemical transformations at low operating temperatures and light intensities makes these photocatalysts ideal for extended use. Mechanistically, localized surface plasmons (LSPs) excited on metal NPs decay nonradiatively into high-energy hot electrons with energies between the vacuum energy and the Fermi level.¹⁵ Hot electrons may then relax through electron–phonon coupling¹⁶ or, in the presence of molecular adsorbates, may scatter into an excited state of the molecule, triggering a chemical reaction by reducing the activation energy. In our previous work⁵ we showed that H₂/D₂ molecules can be dissociated on gold nanoparticle (AuNP) surfaces supported on a TiO₂ matrix, where the activation energy of the dissociation reaction of H₂, 4.5 eV, is reduced to 1.7–1.8 eV by this plasmon-enabled mechanism. The dissociation is enabled by the formation of a transient excited Feshbach resonance,¹⁷ where hot electrons with energies of 1.8 eV or greater can result in a transient population of this state. This was achieved by optical excitation of small (5–30 nm diameter) AuNPs having plasmon resonances between 2.2 and 2.3 eV.

We also demonstrated that TiO₂ (bandgap energy 3–3.2 eV) was not actively taking part in the dissociation reaction, and therefore was not excited; the extent of H₂ spillover into the TiO₂ lattice was found to be negligible. However, it is possible that a 0.9–1 eV Schottky barrier was formed at the AuNP/TiO₂ interface, which could have provided additional active sites on the TiO₂ that could be excited indirectly by incident light,

creating an additional channel for electron transfer. Therefore, performing the H₂ dissociation reaction on an entirely inert dielectric support is essential to demonstrate that the observed dissociation is caused by the hot electrons at the AuNP surface. In this Communication, we report the room-temperature, light-induced dissociation of H₂ on similarly sized (5–30 nm) AuNPs supported on a SiO₂ matrix. We observe that, by changing the support from TiO₂ to SiO₂, the rate of H₂ dissociation increases dramatically. This result provides even stronger evidence that dissociation is indeed taking place on the illuminated AuNP surface, mediated by hot-electron capture by the adsorbate molecules, and that the dielectric support does not actively take part in the chemical reaction.⁵ Furthermore, the reaction was found to be active using Al₂O₃ as a support (Supporting Information S8). This provided additional proof that the reaction is indeed hot-electron-induced and can be performed on any substrate.

To monitor H₂ dissociation, D₂ was also used as a reactant and the product HD was used as the probe molecule, where the overall reaction is H₂(g) + D₂(g) → 2HD(g). The experimental setup was described in our previous work.⁵ First, 1% Au, in the form of colloidal NPs with an average diameter of 13.7 nm supported on SiO₂ (Figure 1A,B), was prepared using a wet chemical deposition precipitation method (sample information provided in the Supporting Information S1). The photocatalyst sample was loaded into a stainless steel reaction chamber (Harrick Scientific) equipped with 1 cm diameter quartz window. Next, 10 sccm of ultrapure H₂ and 10 sccm of D₂ gas (Matheson) were flowed into the chamber. White light from a supercontinuum laser source (Fianium) was filtered and used to excite the AuNP plasmon over a range of intensities and wavelength bands across the visible region of the spectrum.

The rate of HD formation with and without the supercontinuum laser excitation (2.4 W/cm²) on the present Au/SiO₂ is shown in Figure 1C. The photocatalyst was initially kept at 22–24 °C under dark conditions (laser off) while a steady HD background level was obtained.^{4,5,12} Upon laser excitation, the rate of HD formation increased instantaneously by a factor of ~150. Within 10 min of laser excitation, a steady rate was achieved. In addition, the temperature of the sample simultaneously increased by ~8 °C due to laser heating. After 10 min the laser was switched off, which immediately reverted

Received: October 28, 2013

Published: December 19, 2013

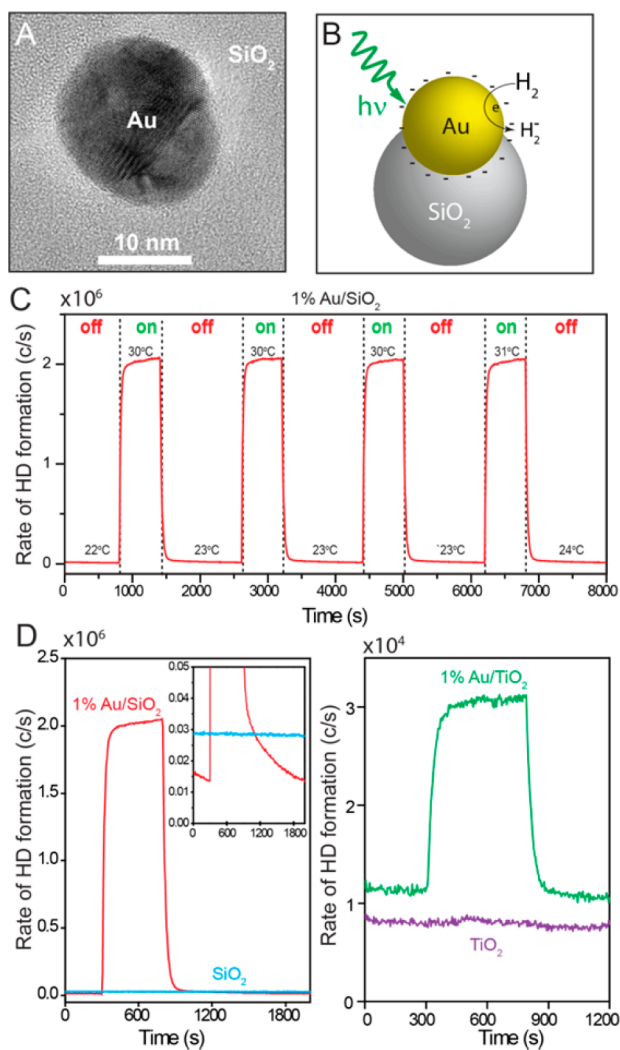


Figure 1. Hot-electron-induced dissociation of H_2/D_2 at room temperature ($\sim 23^\circ\text{C}$) using 1% Au/SiO₂ photocatalyst. (A) High-resolution transmission electron micrograph of a single AuNP supported on SiO₂ matrix showing darker contrast of AuNP as compared to SiO₂ support. (B) Schematic representation of hot-electron-induced dissociation of H_2 on Au. (C) Real-time detection of rate of HD formation with laser excitation (2.4 W/cm^2 , on) and without laser excitation (0.0 W/cm^2 , off). Due to laser heating during 10 min of laser excitation, the temperature on the sample changes reversibly by 8°C , as shown in the figure, from 22 to 30°C . (D) A comparison of the rate of formation of HD using 1% Au/SiO₂ (left panel, red, inset showing the baseline of HD formation) and 1% Au/TiO₂ (right panel, green) at the same experimental conditions and laser intensities (2.4 W/cm^2). No photocatalytic rate was observed with pristine SiO₂ (left panel, blue) and TiO₂ (right panel, purple). The diameters of the AuNPs were $5\text{--}30\text{ nm}$. The excitation wavelength range is $450\text{--}1000\text{ nm}$.

the system to its initial rate and photocatalyst temperature, showing a reversibility of the process.

To demonstrate the efficiency of H_2 dissociation using Au/SiO₂ photocatalyst in direct comparison with the Au/TiO₂ previously used,⁵ the rate of photocatalytic HD formation was monitored on both 1% Au/SiO₂ and 1% Au/TiO₂ (see synthesis method in Supporting Information S1) shown in Figure 1D. Compared to the $\sim 150\times$ rate increase observed for Au/SiO₂, the rate enhancement in the case of Au/TiO₂ was found to occur only by a factor of ~ 2.7 . The much lower rate

obtained for the case of Au/TiO₂ may be due to the fact that the Au–TiO₂ metal–semiconductor junction forms a Schottky barrier with a height of nominally ($0.8\text{--}1\text{ eV}$). Upon laser excitation, the hot electrons with energies greater than the barrier are able to transfer from the AuNP to the TiO₂. This leads to a substantial reduction of the number of hot electrons available for charge transfer into the physisorbed H_2 . However, in case of Au/SiO₂, no such barrier is formed, and more of the hot electrons generated on the AuNP surface can transfer into the physisorbed H_2 . Control experiments were also performed using pristine SiO₂ and TiO₂, which did not show evidence of photocatalysis (Figure 1D).

To confirm that the enhancement of the photocatalytic rate was not due to laser heating, the temperature of the 1% Au/SiO₂ photocatalyst, initially kept at 24°C , was increased to 30°C and eventually to 100°C without laser illumination. This caused a small ($\sim 3.7\times$) increase in the rate of formation of HD, far smaller than the $\sim 150\times$ photocatalytic rate enhancement shown in Figure 2A.

To further demonstrate that local heating on the surface of the AuNP is not responsible for the observed photocatalytic rate, a plasmonic heating model^{5,18–20} was used to calculate the temperature increase (ΔT) on the surface of individual AuNPs.

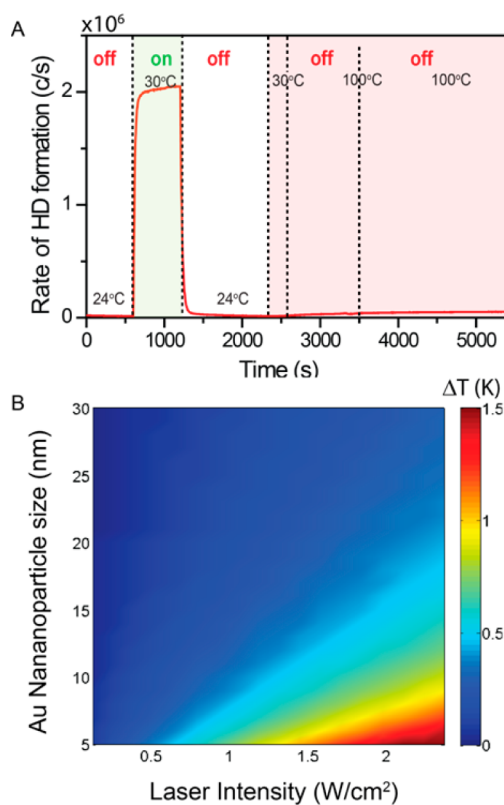


Figure 2. Effect of plasmonic and laser heating. (A) Distinction between the photocatalytic rate (laser only) and thermal heating rate (heat only). The shaded gray area displays the photocatalytic rate of HD formation on the AuNP use in Figure 1 for laser intensity of 2.4 W/cm^2 . The excitation wavelength range is $450\text{--}1000\text{ nm}$. The shaded red area displays the rate of HD formation due to heating of the photocatalyst sample from room temperature (24°C) to 31°C and ultimately 100°C as well under dark conditions. (B) Increase in local temperature of individual, well-separated AuNP of different sizes ($5\text{--}30\text{ nm}$ AuNP) embedded in SiO₂ matrix as a function of laser intensities, showing negligible increase in temperature.

Isolated AuNPs were simulated as being half-embedded inside a SiO₂ matrix. The local change in temperature on the AuNP due to plasmonic heating can be expressed as

$$\Delta T = \frac{\sigma_{\text{abs}} I}{4\pi R \beta \kappa_m} \quad (1)$$

where σ_{abs} is the integrated absorption cross section over the entire visible range (450–1000 nm), I is the laser intensity, R is the radius of the spherical AuNP, β is the thermal capacitance coefficient depending on the NP aspect ratio ($\beta = 1 + 0.96587[\ln^2(\text{AR})]$, $\beta = 1$ for a spherical NP), and κ_m denotes the temperature-dependent thermal conductivity of the surrounding dielectric (SiO₂).²¹ Finite-difference time-domain (FDTD) simulations were performed to calculate the absorption cross sections of the 1% Au/SiO₂ photocatalyst. Calculations were performed on single spherical AuNPs semi-embedded into a SiO₂ matrix under longitudinally polarized excitation. Johnson and Christy²⁰ and Palik²² dielectric functions were used for Au and SiO₂, respectively. Absorption spectra were calculated for AuNP sizes ranging from 5 to 30 nm. A contour plot with ΔT as a function of laser intensity and a series of AuNP sizes shows only a nominal 1.5 K rise in surface temperature with 2.5 W/cm² of laser of excitation (Figure 2 and Supporting Information S7). This shows that photothermal heating is not the cause of the observed HD formation. The relatively low plasmon-induced temperature increase of the AuNP is due to the low laser intensities used and the small absorption cross sections of small AuNPs. It is observed that the local change in AuNP surface temperature due to plasmonic heating in the case of Au/SiO₂ dielectric support is more pronounced (~ 1.5 K at 6 nm diameter AuNP at 2.5 W/cm² laser intensity) than with Au/TiO₂ support (~ 0.5 mK only with 6 nm diameter AuNP at 2.5 W/cm² laser intensity). The increased plasmonic heating also contributes to increased generation of hot electrons on the AuNP surface.²³

The intensity dependence of the rate of HD formation for 1% Au/SiO₂ at a constant temperature of 100 °C is shown in Figure 3A. We observe a clear linear dependence of the photocatalytic rate on excitation laser intensity. This linear dependence supports our understanding that the rate of photocatalysis is dominated by conversion of single photons to single hot electrons which initiate a single H₂ dissociation event.

The wavelength dependence on photocatalytic rate is shown in Figure 3B. The 1% Au/SiO₂ photocatalyst was kept at 100 °C to avoid any thermal fluctuations due to laser heating. Fifteen band-pass filters (Edmund Optics, Interference filters) having transmission maxima at wavelengths separated by 25 nm were used. The transmitted output intensity of laser light was adjusted to 130 mW/cm². The wavelength dependence of HD formation, with a prominent shoulder at 590 nm, differs substantially from the experimental diffuse reflectance spectrum which peaks at nominally 525 nm (see Supporting Information S5 and S6). The spectral difference between the HD formation rate and the reflectance spectrum of the Au/SiO₂ may be attributable to the reduction of SiO₂ to Si–O(H)–Si during the course of the reaction. After H₂/D₂ is photocatalytically dissociated on the AuNP surface, the atomic species may get incorporated into the oxide support by spillover and diffusion across the metal–oxide interface,^{24–26} resulting in the conversion of SiO₂ to SiO:H.^{27–29} The substantial increase in refractive index from SiO₂ ($n = 1.5$) to Si–O(H)–Si ($n = 2.2$ –

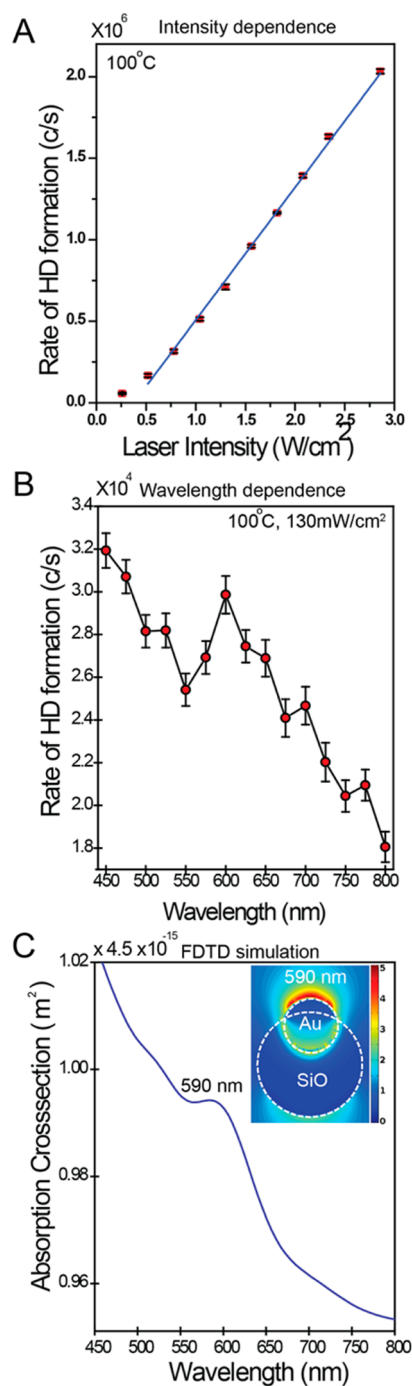


Figure 3. Dependence of photocatalytic rate on the intensity and wavelength of laser excitation for the AuNP used in Figures 1 and 2. (A) Rate of formation of HD (laser on) as a function of intensity of laser excitation using 1% Au/SiO₂ kept at fixed temperature of 100 °C. Linear intensity dependence is observed. (B) Rate of HD formation at 100 °C as a function of band-pass filter wavelength, each adjusted to an intensity of 130 mW/cm² using 1% Au/SiO₂. Error bars in (A) and (B) were calculated as the standard deviation of the instrumental fluctuations in rate measurements using the quadrupole mass spectrometer. (C) Simulated absorption cross section spectrum of Au/SiO photocatalyst sample, modeled as 10 nm AuNP 75% embedded into a 40 nm SiO₂ NP. It features a dipole mode located at 590 nm. Inset shows the local field enhancement $|E/E_0|^2$.

2.5)³⁰ may be responsible for the large red shift and spectral distortion of the observed wavelength dependence of HD

formation relative to the diffuse reflection spectrum of the unused photocatalyst.

To account for the observed wavelength dependence of the action spectrum, FDTD simulations were performed with a 10 nm AuNP 75% embedded by volume inside a 40 nm SiO₂ NP with a refractive index of 2.5.³¹ The calculated absorption spectrum (Figure 3C) exhibits a dipolar LSP resonance at 590 nm, in excellent agreement with the peak observed in the HD formation rate spectrum (Figure 3B). A near-field enhancement ($|E/E_0|^2$) contour plot is shown as an inset, to illustrate the nature of the LSP resonance and to display the geometry used in the simulations.

In summary, we have observed plasmon-induced H₂/D₂ dissociation on AuNPs supported on dielectric SiO₂ and Al₂O₃ NPs. In comparison to our previous study of H₂ dissociation on AuNPs on TiO₂, the reaction rate in the presence of SiO₂ is enhanced by almost 2 orders of magnitude. This result strongly supports the proposed mechanism that hot electrons generated by plasmon decay transfer to the H₂ molecules, substantially reducing the barrier for H₂ dissociation. The result supports our earlier conclusion that the dielectric support plays a passive role in this reaction process. A plausible explanation for the substantially larger dissociation rate in the presence of an SiO₂ relative to TiO₂ NP support is the presence of a Schottky barrier at the AuNP/TiO₂ surface, which may facilitate hot-electron transfer into the TiO₂ matrix, reducing the number of electrons available for the H₂ dissociation. We also observed the transient effect of spillover of atomic species into the SiO₂ matrix, an effect which was inferred from the spectral shift of the action spectrum in situ due to local dielectric change of the support. This H₂ dissociation process on dielectric support may prove to provide a low-temperature alternative photoinduced reaction pathway for all-optical control of chemical transformation.

■ ASSOCIATED CONTENT

📄 Supporting Information

Au/SiO₂ photocatalyst sample preparation, characterization of structure and morphology, spectroscopic characterization, and H₂ dissociation using Au@Al₂O₃. This material is available free of charge via the Internet at <http://pubs.acs.org>.

■ AUTHOR INFORMATION

Corresponding Authors

nordland@rice.edu

halas@rice.edu

Author Contributions

[§]S.M. and L.Z. contributed equally to this work.

Notes

The authors declare no competing financial interest.

■ ACKNOWLEDGMENTS

This work was supported by the U.S. Air Force Office of Scientific Research (AFOSR) FA9550-10-1-0469, the Robert A. Welch Foundation under grants C-1220 and C-1222, and the Cyberinfrastructure for Computational Research funded by NSF under grant CNS-0821727.

■ REFERENCES

- (1) Linic, S.; Christopher, P.; Ingram, D. B. *Nat. Mater.* **2011**, *10*, 911.
- (2) Hou, W. B.; Cronin, S. B. *Adv. Funct. Mater.* **2013**, *23*, 1612.

- (3) Liu, Z. W.; Hou, W. B.; Pavaskar, P.; Aykol, M.; Cronin, S. B. *Nano Lett.* **2011**, *11*, 1111.
- (4) Christopher, P.; Xin, H.; Linic, S. *Nat. Chem.* **2011**, *3*, 467.
- (5) Mukherjee, S.; Libisch, F.; Large, N.; Neumann, O.; Brown, L. V.; Cheng, J.; Lassiter, J. B.; Carter, E. A.; Nordlander, P.; Halas, N. J. *Nano Lett.* **2012**, *13*, 240.
- (6) Marimuthu, A.; Zhang, J. W.; Linic, S. *Science* **2013**, *339*, 1590.
- (7) Zhao, Z. Y.; Carpenter, M. A. *J. Phys. Chem. C* **2013**, *117*, 11124.
- (8) Mubeen, S.; Singh, N.; Lee, J.; Stucky, G. D.; Moskovits, M.; McFarland, E. W. *Nano Lett.* **2013**, *13*, 2110.
- (9) Mubeen, S.; Lee, J.; Singh, N.; Kramer, S.; Stucky, G. D.; Moskovits, M. *Nat. Nanotechnol.* **2013**, *8*, 247.
- (10) Pineda, A.; Gomez, L.; Balu, A. M.; Sebastian, V.; Ojeda, M.; Arruebo, M.; Romero, A. A.; Santamaria, J.; Luque, R. *Green Chem.* **2013**, *15*, 2043.
- (11) Wu, X. M.; Thrall, E. S.; Liu, H. T.; Steigerwald, M.; Brus, L. J. *Phys. Chem. C* **2010**, *114*, 12896.
- (12) Christopher, P.; Xin, H.; Marimuthu, A.; Linic, S. *Nat. Mater.* **2012**, *11*, 1044.
- (13) Linic, S.; Christopher, P.; Xin, H.; Marimuthu, A. *Acc. Chem. Res.* **2013**, *46*, 1890.
- (14) Brus, L. *Acc. Chem. Res.* **2008**, *41*, 1742.
- (15) Govorov, A. O.; Zhang, H.; Gun'ko, Y. K. *J. Phys. Chem. C* **2013**, *117*, 16616.
- (16) Aruda, K. O.; Tagliacuzzi, M.; Sweeney, C. M.; Hannah, D. C.; Schatz, G. C.; Weiss, E. A. *Proc. Natl. Acad. Sci. U.S.A.* **2013**, *110*, 4212.
- (17) Libisch, F.; Cheng, J.; Carter, E. A. *Z. Phys. Chem.* **2013**, *227*, 1455.
- (18) Baffou, G.; Quidant, R.; Girard, C. *Appl. Phys. Lett.* **2009**, *94*, 153109.
- (19) Govorov, A. O.; Richardson, H. H. *Nano Today* **2007**, *2*, 30.
- (20) Johnson, P. B.; Christy, R. W. *Phys. Rev. B* **1972**, *6*, 4370.
- (21) Fang, J.; Huang, Y.; Lew, C. M.; Yan, Y.; Pilon, L. *J. Appl. Phys.* **2012**, *111*, 054910.
- (22) Philipp, H. R. In *Handbook of Optical Constants of Solids*; Edward, D. P., Ed.; Academic Press: Burlington, 1997; p 749.
- (23) Lee, Y. K.; Jung, C. H.; Park, J.; Seo, H.; Somorjai, G. A.; Park, J. Y. *Nano Lett.* **2011**, *11*, 4251.
- (24) Lenz, D. H.; Conner, W. C., Jr. *J. Catal.* **1987**, *104*, 288.
- (25) Conner, W. C.; Falconer, J. L. *Chem. Rev.* **1995**, *95*, 759.
- (26) Valerii, V. R.; Oleg, V. K. *Russ. Chem. Rev.* **1997**, *66*, 107.
- (27) Jabłoński, J. M.; Okal, J.; Potoczna-Petru, D.; Krajczyk, L. *J. Catal.* **2003**, *220*, 146.
- (28) McTaggart, F. K. *Nature* **1964**, *201*, 1320.
- (29) Han, G.; Sohn, H. Y. *J. Am. Ceram. Soc.* **2005**, *88*, 882.
- (30) Arup, S.; Debajyoti, D. *J. Phys. D: Appl. Phys.* **2009**, *42*, 215404.
- (31) Hass, G.; Salzberg, C. D. *J. Opt. Soc. Am.* **1954**, *44*, 181.